Carbon Black-Filled Poly(ethylene-*co*-alkyl acrylate) Composites: Calorimetric Studies

J. F. FELLER, I. LINOSSIER, S. PIMBERT, G. LEVESQUE

Laboratoire Polymères & Procédés, Université de Bretagne-Sud, Rue de Saint-Maudé, 56 325 Lorient, France

Received 25 October 1999; accepted 17 March 2000

ABSTRACT: The calorimetric characteristics of carbon black (CB)/poly(ethylene-*co*-alkyl acrylate) composites depend on both the CB and acrylate contents. An increase of the acrylate content in the pure copolymers tends to decrease all the crystalline characteristics: $T_{c,n}$, the nonisothermal crystallization temperature; T_m, the melting temperature, and ΔH_m, the melting enthalpy. CB modifies the crystallization kinetics of poly(ethylene-*co*-ethyl acrylate) (EEA) alone and in blends with poly(ethylene-*co*-24% w/w methyl acrylate) (24EMA) and poly(ethylene-*co*-35% w/w methyl acrylate) (35EMA). In the presence of CB, $T_{c,n}$, the nonisothermal crystallization temperature of EEA, increases and $t_{1/2}$, the half-crystallization time, decreases for a given isothermal crystallization temperature, $T_{c,i}$. The thermograms obtained during the melting of EEA after isothermal crystallization show multiple endotherms, suggesting that crystalline-phase segregation has occurred. The existence of different crystalline species can be explained by the presence of fractions of different acrylate content in the copolymers as shown by SEC. Therefore, CB does not seem to have much effect on the subsequent melting temperature of EEA, $T_{m,s}$. CB also induces a lower melting enthalpy, ΔH_m, in the blends. This decrease of ΔH_m appears to be constant whatever the compound, but when reported to the melting enthalpy of the polymer without CB, $\delta\Delta H_m/\Delta H_m$ increases with the acrylate content. A slight increase of the amorphous phase stiffness after CB introduction is noticed: The T_g of EEA/24EMA and EEA/35EMA blends increases by several degrees. Therefore, plotting ΔH_m versus ΔC_p shows that for the same ΔH_m the ΔC_p is lower in CB-filled samples, suggesting there is some kind of rigid amorphous phase not contributing to the glass transition. We propose to explain the CB activity during the crystallization process by the existence of molecular interactions between CB and acrylate groups rather than by a pure nucleating effect. Thus, the increase of $T_{c,n}$ and the decrease of ΔH_m could be explained by the fact that CB separates acrylate-rich chains from the crystallization medium, accelerating the crystallization of the acrylate-poor chains. During such a crystallization process, CB may be preferentially localized in the more polar amorphous phase and scattered between the two crystalline phases of EEA and EXA. These blends of poly(ethylene-*co*-alkyl acrylate) copolymers with CB provide interesting materials with adjustable properties depending on the acrylate and CB contents and on the thermomechanical treatments. © 2000 John Wiley & Sons, Inc. J Appl Polym Sci 79: 779–793, 2001

Key words: crystallization; poly(ethylene-*co*-alkyl acrylate) blends; CB; nucleation; phase segregation

Correspondence to: J. F. Feller (jean-francois.feller@univ-ubs.fr).

Contract grant sponsor: French Ministry of Research; contract grant number: UPRES 2592.

Journal of Applied Polymer Science, Vol. 79, 779–793 (2001)

INTRODUCTION

Numerous studies have been carried out on carbon-black (CB)-filled polyolefin blends. Most of them focused on the so-called positive temperature coefficient (PTC) phenomenon,[1–5] which is characterized by a nonlinear variation of the composite's electrical resistivity with temperature. A sudden increase in resistivity is observed when the CB concentration in the composite is close to the percolation threshold. The temperature effect on the structure is thought to disconnect the conductive particles or aggregates and, as a consequence, to prevent the current circulation. This phenomenon particularly depends on the CB nature, structure, and content.[2,5,6,7] It is generally accepted that one of the most important factors governing the PTC effect is the thermal expansion coefficient variation during the phase transition of the polymer matrix.[5,8–10] However, the percolation theory is only one of several theories proposed to describe the PTC effect (conduction pathway, electric field emission, tunnel effect double percolation[11,12]) and may not explain alone all the encountered phenomena. The good results generally obtained with semicrystalline polyolefins to design switching materials is certainly due to their crystalline structure, but, moreover, to the CB distribution in the structure which determines the morphology of the conductive path.[10–13] The organization of CB particles in the composite depends on the thermomechanical processing conditions and, particularly, on the influence of crystallization on the particle migration and interactions.[7,11–14]

Carbon black-filled (CB) polymer formulations are often processed by mixing a CB-containing masterbatch with other desirable materials (polymers and copolymers). As the nature and morphology of polymer phases play essential roles in the conductive properties of such formulations, it seemed interesting to examine such blends. This article describes results obtained from a calorimetric study of several polyolefin blends containing CB.

Table I Poly(ethylene-*co*-ethyl acrylate), EEA, and EEA-C Used

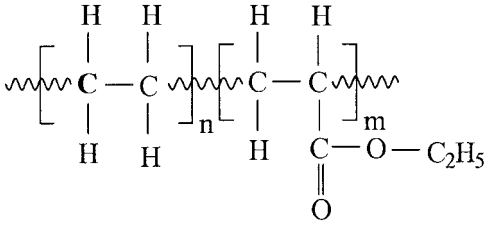

Table II Poly(ethylene-*co*-methyl acrylate), 9EMA, 18EMA, 24EMA, and 35EMA Used

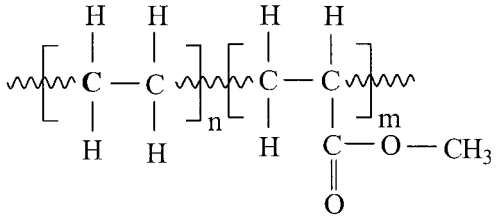

EXPERIMENTAL

Materials and Sample Preparation

Low-density polyethylene (LDPE; LACQTENE 1200 MN26) and all poly(ethylene-*co*-methyl acrylate) (EMA) and poly(ethylene-*co*-butyl acrylate) (EBA) copolymers were kindly supplied by Elf Atochem (Lyon; see Tables I–IV). Acrylate contents in these copolymers are between 7 and 35% (in weight). The producer values were checked by ^{1}H-NMR measurements for three products (24EMA, 35EMA, and EEA-C in C_6D_6) and found to be in good agreement. Poly(ethylene-*co*-methyl acrylate) (EEA) and CB-filled EEA (abbreviated EEA-C, referenced as LE 7704) were obtained from Borealis (Zwijndredt, Belgium). EEA-C contains 63% of EEA and 37% of CB (w/w). All blends were prepared by dissolution in toluene at 80°C under stirring, followed by precipitation in a large volume of ethanol at ambient temperature and subsequent filtration. The blends were dried for 24 h at 50°C in an air-pulsed oven and stored in sealed boxes until analysis. Ethylene/acrylate copolymers are synthesized by free-radi-

Table III Poly(ethylene-*co*-butyl acrylate), 7EBA, 17EBA, and 35EBA Used

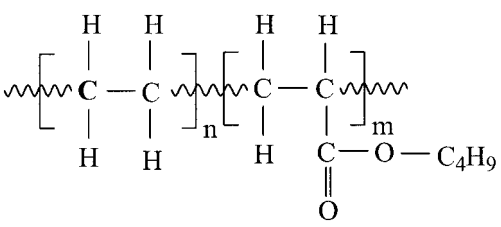

Table IV Thermal Characteristics of the Copolymers

Parameter	LDPE	7EBA	9EMA	EEA	17EBA	18EMA	24EMA	35EBA	35EMA
Alkyl acrylate content[a]	0	1.62	3.3	4.29	4.43	6.88	10.03	10.54	13.52
Alkyl acrylate content[b]	0	6–8	8.5–10.5	13.8	16–19	17–20	25.5	33–37	32.5
T_g (°C)	—	—	—	−33	—	—	−28	—	−30
T_m (°C)[c]	113	103.5	101.5	99.5/75	96.5/83	85/69	76/61	66/48	62/26
$T_{c,n}$ (°C)[d]	98.5/61	88	86	83	79/49	67/44	57/38	48	40
ΔH_m (J g^{-1})	132.5	100.5	83	63	73	55	29.5	11.5	8
Melt-flow index[e]	11.2–11.8	1–1.5	1.8–2.6	6.8–7.0	3.5–4.5	2–3	0.4–0.6	35–45	4.5–6

[a] Molar % calculated from % w/w (except EEA, 24EMA, and 35EMA determined from ^{1}H-NMR spectra.
[b] % w/w range from producer (except EEA, 24EMA, and 35EMA calculated from molar %).
[c] First figures correspond to the main peak and the second, to the shoulder.
[d] Nonisothermal crystallization temperature.
[e] MFI range from producer (except LDPE and EEA determined with a melt indexer) according to ASTM D 1238.

cal polymerization, providing a statistic structure to these copolymers. This synthesis leads to chain families with different molar masses, evidenced by SEC measurements on 35EMA in THF. In Figure 1, three peaks (or shoulders) of increasing size from left to right can be seen; they are centered, respectively, on the following masses: $M_w = 2.367 \times 10^6$ g mol^{-1}, M_w = 545,000 g mol^{-1}, and M_w = 72,000 g mol^{-1}. Buback et al.[15–17] recently studied the polymerization conditions of such products and determined accurate values of the copolymerization reactivity parameters for ethylene and several alkyl acrylates, which suggests that this way of synthesis provides chain populations of different acrylate contents.

Equipment and Experiments

Thermograms were obtained on a Perkin–Elmer Pyris 1 differential scanning calorimeter (DSC) using the Pyris V 3.0 software under Windows NT 4.0 for data collection and treatment. This apparatus has a sensitivity of 0.2 μW, a precision of temperature of 0.01°C, and a precision of heat flow better than 0.1%. This allows small amplitude phenomenon detection, which is the case in

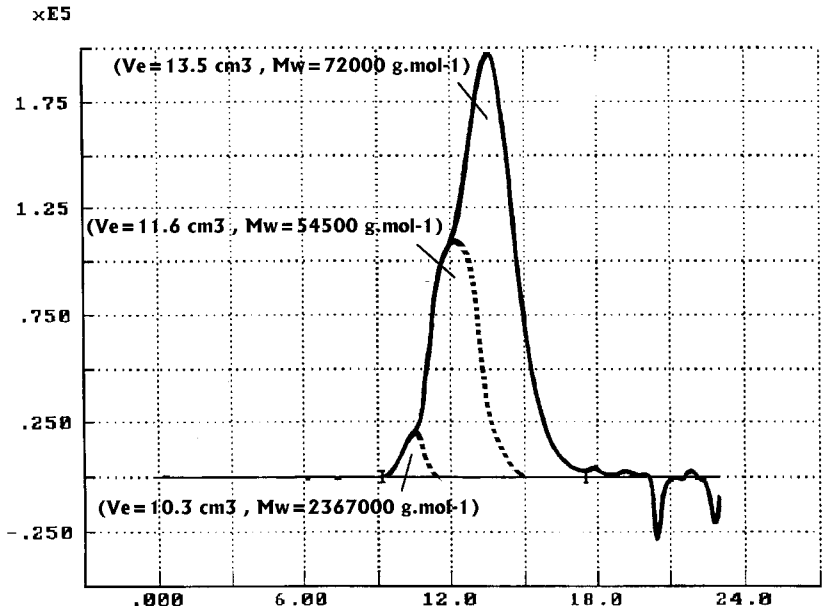

Figure 1 SEC molar mass measurements obtained for 35EMA.

the study. The calibration was done with indium and zinc in the temperature range +15 to +350°C under cooling with a simple cryostat and with cyclohexane and indium for the range −50 to +200°C when the DSC was cooled by a "cryofil" using liquid nitrogen. The baseline was checked every day. Aluminum pans with holes were used and the samples mass was approximately 10 mg. All samples were first heated to 150°C for 5 min to get rid of the thermal history and, eventually, solvent traces (although FTIR spectra showed that drying was effective). All the temperatures measured from a peak extremum (T_c, T_m) were determined at less than ±0.5°C and from a sigmoid (T_g) at less than ±1°C.

Nonisothermal crystallization and melting temperatures, respectively, $T_{c,n}$ and T_m, were determined from the crystallization peak extrema in experiments at ±10°C min^{-1} heating/cooling rates. Subsequent melting temperatures were obtained by the melting peaks' maxima measured at a 20°C min^{-1} heating rate. Melting enthalpies were determined using constant integration limits (when possible) and corrected for CB content (if needed). Isothermal crystallization from the melt was performed for 60 min after quenching at a −90°C min^{-1} cooling rate. The half-crystallization times, $t_{1/2}$, were determined using the extrema of the crystallization exotherms (if symmetrical and using a baseline subtraction) for times under 1 min and with the half-width point for 50% crystalline conversion for times over 1 min. The glass transition temperatures were determined at half-heat capacity variation ($\frac{1}{2}\Delta C_p$) during heating from −125 to 125°C at 40°C min^{-1} (after quenching at −200°C min^{-1}). ΔC_p is determined from the baseline slope difference after and before the glass transition. FTIR spectra were obtained on a Perkin–Elmer Spectrum 1000 spectrometer.

RESULTS AND DISCUSSION

This article reports on blends of an ethylene/ethyl acrylate copolymer (a commonly used matrix in CB-containing masterbatches) with other polyolefins such as LDPE or other ethylene/alkyl acrylate copolymers. These formulations were examined with and without CB. The use of power-compensation DSC allows the study of the CB influence on the nature and properties of the crystalline and amorphous phases formed during the blending process. For convenience, all ethylene/alkyl acrylate copolymers are designated as EXA (generic abbreviation for EBA, EEA, and EMA).

EXA Thermal Behavior

Nonisothermal experiments were carried out on the different EXAs to identify their characteristic temperatures and enthalpies.

EXA Crystallization Temperatures

The nonisothermal crystallization temperature ($T_{c,n}$) of the ethylene/acrylate copolymers gradually decreases with increasing acrylate concentration in the copolymers (Fig. 2). This induces a decrease in the mean crystallizable sequence length, leading to thinner lamellas.[18–22] Three types of acrylate copolymers with various molar contents were studied: EEA (4.29%), EBAs (1.62, 4.43, and 10.54%), and EMAs (3.30, 6.88, 10.03, and 13.55%). Each series fits a linear law quite well in the considered range. Thus, it can be seen that the evolution of $T_{c,n}$ versus the acrylate content is quite independent of the acrylate nature and that an increase in the acrylate content from 3 to 13% induces a decrease of approximately 50°C of $T_{c,n}$.

EXA Melting Temperatures

The EXA melting temperatures decrease with an increasing acrylate concentration in the copolymer (Fig. 3). The introduction of acrylate comonomers (considered as defects toward crystallization and rejected from the crystals) decreases the lamella thickness, causing a decrease in the melting temperature. The same regular evolution as for $T_{c,n}$ is observed for T_m; T_m is located about 20°C above $T_{c,n}$.

EXA Melting and Crystallization Enthapies

Another aspect of this preliminary study concerns melting and crystallization enthalpies. Important variations in both crystallization and melting enthalpies related to the acrylate content in EXA are noticed in Figure 4. ΔH decreases from 100 to 10 J g^{-1} as the acrylate content is increased from 1.5 to 13.5 (% mol). The same crystallinity loss resulting from the introduction of comonomers was also observed, for example, with poly(propene-*co*-diene)[18] and it was found that the crystallinity $\Delta H_m/\Delta H^0_m$ decreased from 60 to 10%, with the comonomer molar content increasing from 0.5 to 14.5%. This preliminary study clearly evidenced the link between the acrylate content

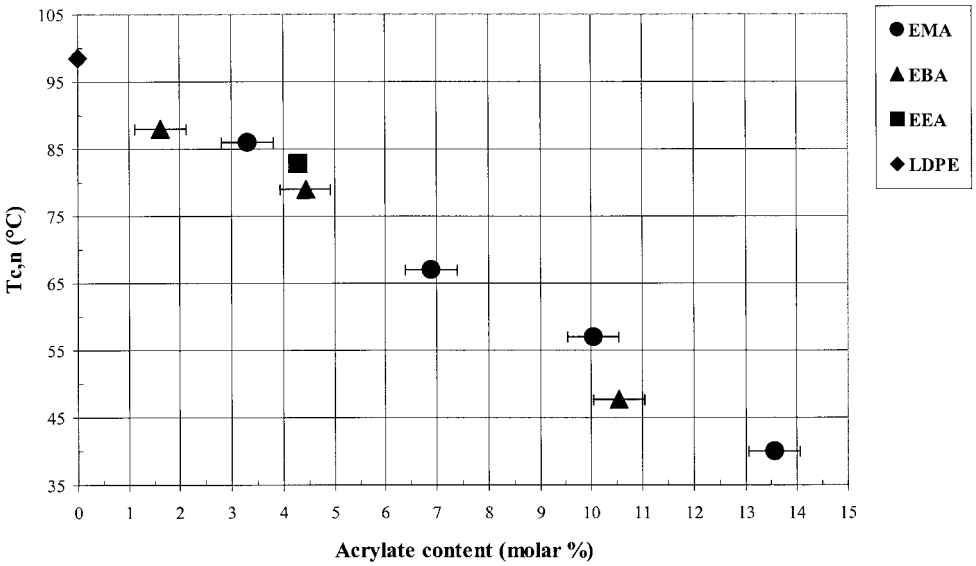

Figure 2 EXAs nonisothermal crystallization temperatures $T_{c,n}$ as a function of the acrylate content (molar %) in the copolymer (cooling rate 10°C min^{-1}).

and the different crystallization characteristic parameters, $T_{c,n}$, T_m, and ΔH, of the copolymers.

Influence of CB on the Blends' Crystalline-phase Properties

EEA/EXA and EEA-C/EXA Blends' Nonisothermal Crystallization Temperature

A nonisothermal crystallization study was carried out on blends of poly(ethylene-*co*-ethyl acrylate) with 37% (weight-to-weight) CB content (EEA-C) and two different poly(ethylene-*co*-methyl acrylate)s, respectively: 25.5% (w/w) and 32.5% (w/w) of acrylate (24EMA and 35EMA). The influence of CB on the nonisothermal crystallization temperature is well illustrated for EEA in Figure 5. One can see an increase of about 5° in the EEA's crystallization temperature $T_{c,n}$ in the presence of CB. This change could be attributed to a CB nucleation effect, which speeds up the crystallization's first step, that is, the nucleation, as it was well evidenced elsewhere.[23] Figure 5 also shows that the shapes of the two curves are quite different. Although a quantitative comparison of EEA-C and EEA enthalpies cannot be done directly, because EEA-C contains 37% in mass of CB, one

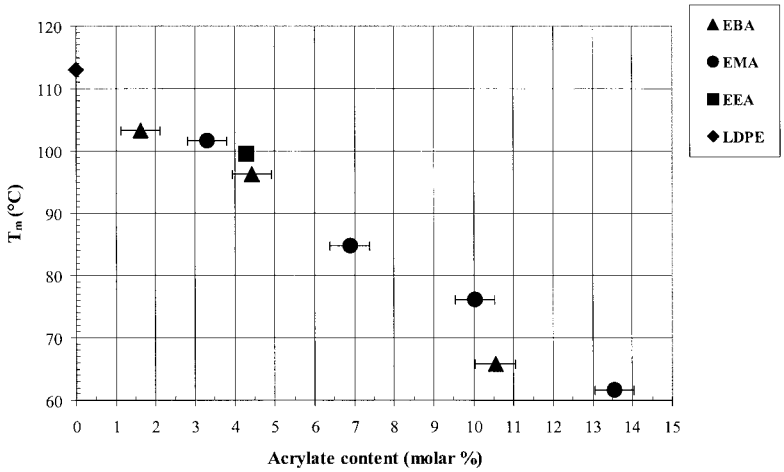

Figure 3 EXAs' melting temperature T_m as a function of the acrylate content (molar %) in the copolymer (cooling rate 10°C min^{-1}).

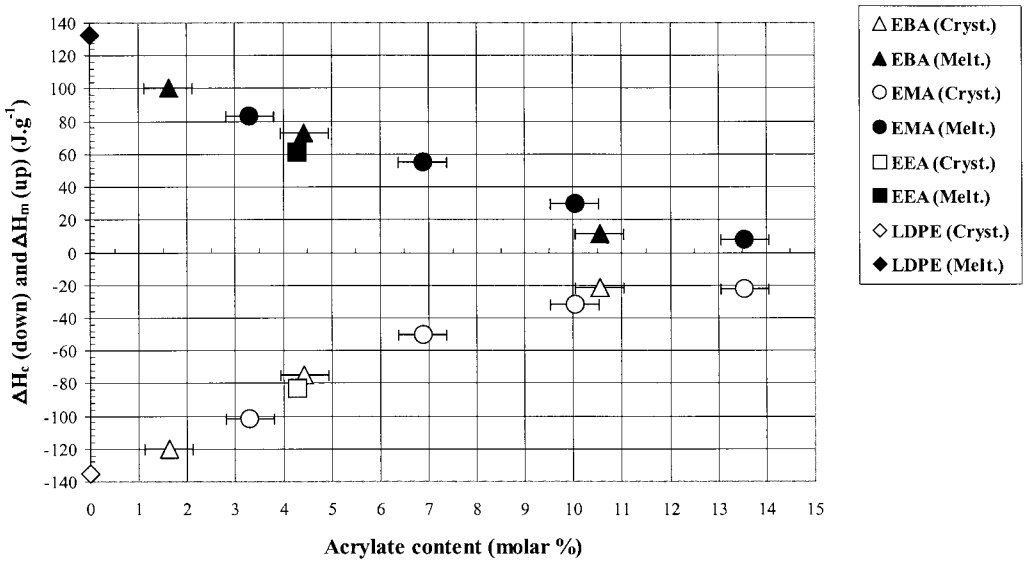

Figure 4 EXAs' melting and crystallization enthalpies ΔH_m and ΔH_c as a function of the acrylate content (molar %) in the copolymer (cooling rate 10°C min^{-1}).

can see that EEA-C's exotherm is broader than that of EEA, suggesting a more progressive process. In the following, the EEA-C's enthalpy calculated by integration of the corresponding exotherm is corrected for the CB content. It is now clear that CB influences the pure copolymer's crystallization and it is interesting to determine if it is also the case in blends.

A typical example of crystallization behavior is shown in Figure 6 for blends of EEA 25%/24EMA 75% (lower curve) and EEA 25.2%/14.8% CB/60% 24EMA (higher curve). These two blends were chosen because they have quite the same EEA and 24EMA contents, so that the shape of the exotherms can be compared. In fact, the blends' composition after correction for CB % is the fol-

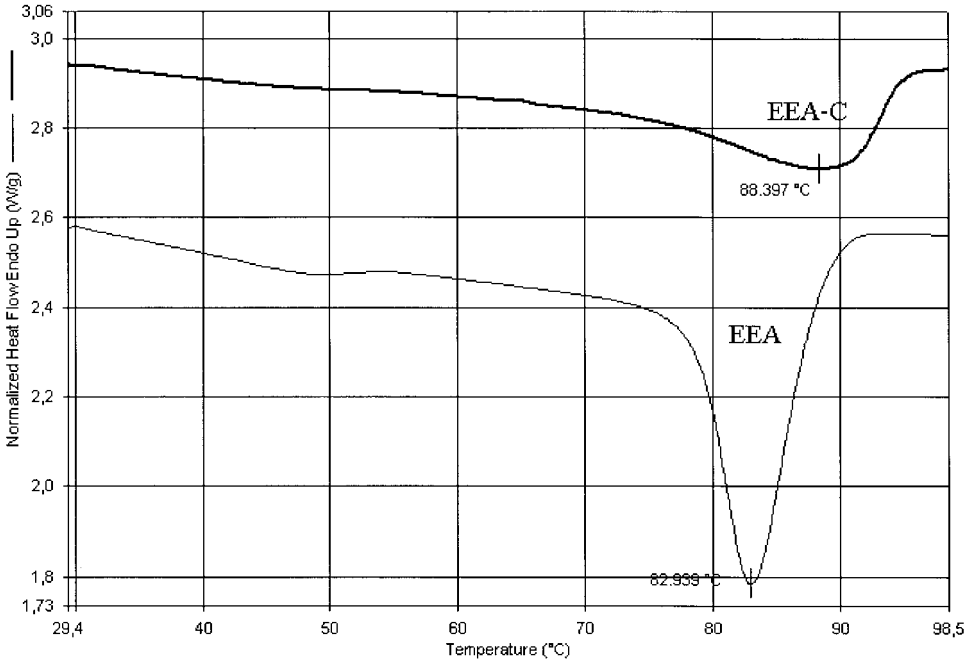

Figure 5 Typical DSC crystallization exotherms obtained for EEA and EEA-C at 10°C min^{-1}).

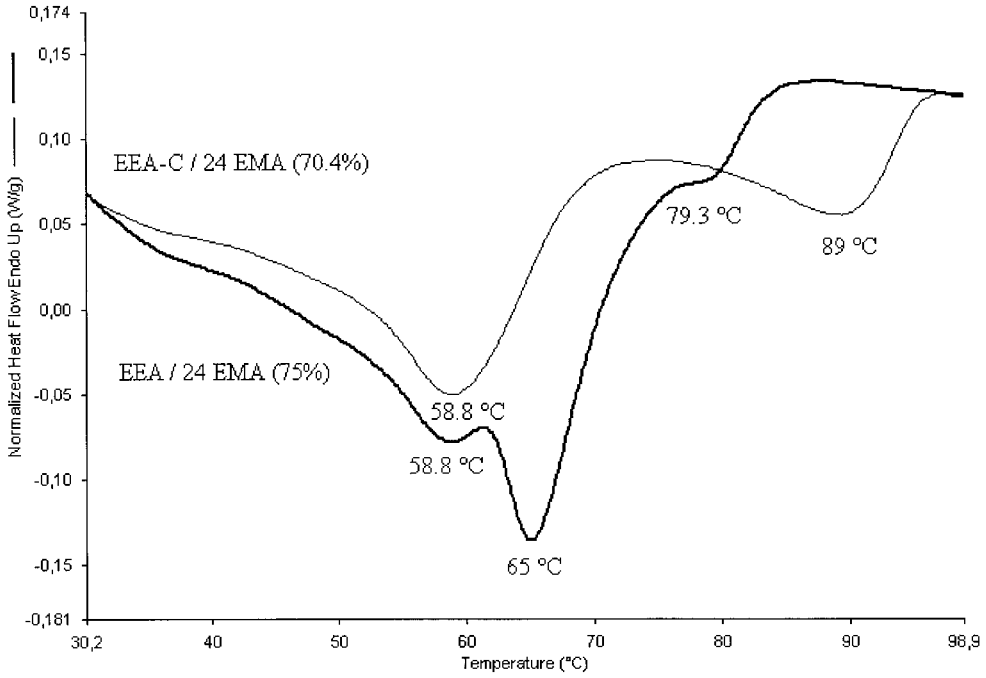

Figure 6 DSC crystallization multiple exotherms observed for EEA-C/24EMA and EEA/24EMA at $-10°C\ min^{-1}$ (cooling rate).

lowing: 29.6% of EEA and 70.4% of 24EMA for the blend with CB and 25% of EEA and 75% of 24 EMA for the blend without CB. Semicrystalline polymers are generally incompatible in the crystalline phases (excepted for some rare cases of cocrystallization[21,24–28] observed when both chemical and crystalline structures are very similar), so that it is not surprising to find several exotherms on the blend thermograms. The analysis of the DSC curves such as shown in Figure 6 leads to results expressed in Figure 7 for blends with 24EMA and in Figure 8 for blends with 35EMA.

Figure 7 shows that, for a given blend, one to three crystallization steps are observed successively which can be associated to chain families of different acrylate content and of different average molar mass previously encountered with SEC. The first crystallization step close to 85°C is attributed to EEA (1), another one near 60°C is attributed to 24EMA (3), and the last one close to 50°C is attributed again to EEA (4). Figure 6 shows an exotherm at 65°C attributed to EEA (2), which was not observed for the other blends. In Figure 8, two crystallization exotherms are seen: the first one close to 85°C is attributed to EEA and the second close to 40°C is attributed to 35EMA.

The presence of multiple exotherms makes the interpretation of the CB nucleating effect in blends more complicated than for single compounds, but several points can be established from Figures 7 and 8:

(a) There is a larger shift in the EEA crystallization temperature than there is for EMA copolymers. In fact, the EMA crystallization temperature is almost unmodified, whereas the CB increases the EEA crystallization temperature from 5 to 10 degrees, as observed for pure EEA.
(b) This larger shift in crystallization temperature encountered for EEA shows that CB speeds up the crystallization of the more crystalline copolymer, which is also the copolymer of a higher crystallization temperature and of a lower acrylate content.
(c) There are fewer exotherms in CB-containing blends. Moreover, CB broadens the exotherms corresponding to EEA crystallization (as in Fig. 5). This suggests that CB either prevents some species from crystallizing or has a compatibilizing effect.
(d) To try to explain the fact that CB does not much influence the EMA crystalline phase, it can be hypothesized that EEA first crystallizes, that is, at a higher temperature, providing a crystalline network that may reduce the motion of CB and EMA chains not already crystallized.

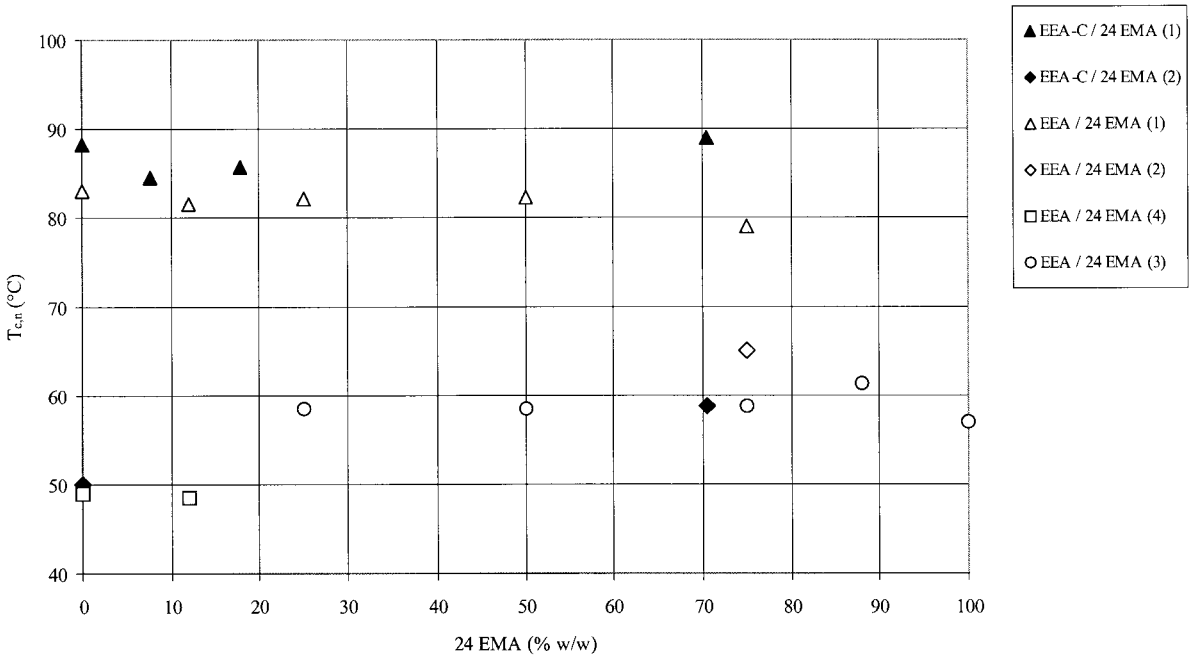

Figure 7 Nonisothermal crystallization temperature evolution in 24EMA/EEA blends with and without CB.

EEA Half-crystallization Time

While the effect of CB on EEA's nonisothermal crystallization is evidenced, the same phenomenon is expected in isothermal crystallization. Actually, Figure 9 shows that at each crystallization temperature the time necessary for half-crystallization, $t_{1/2}$, decreases with the introduction of CB, confirming an increase of the crystallization rate.

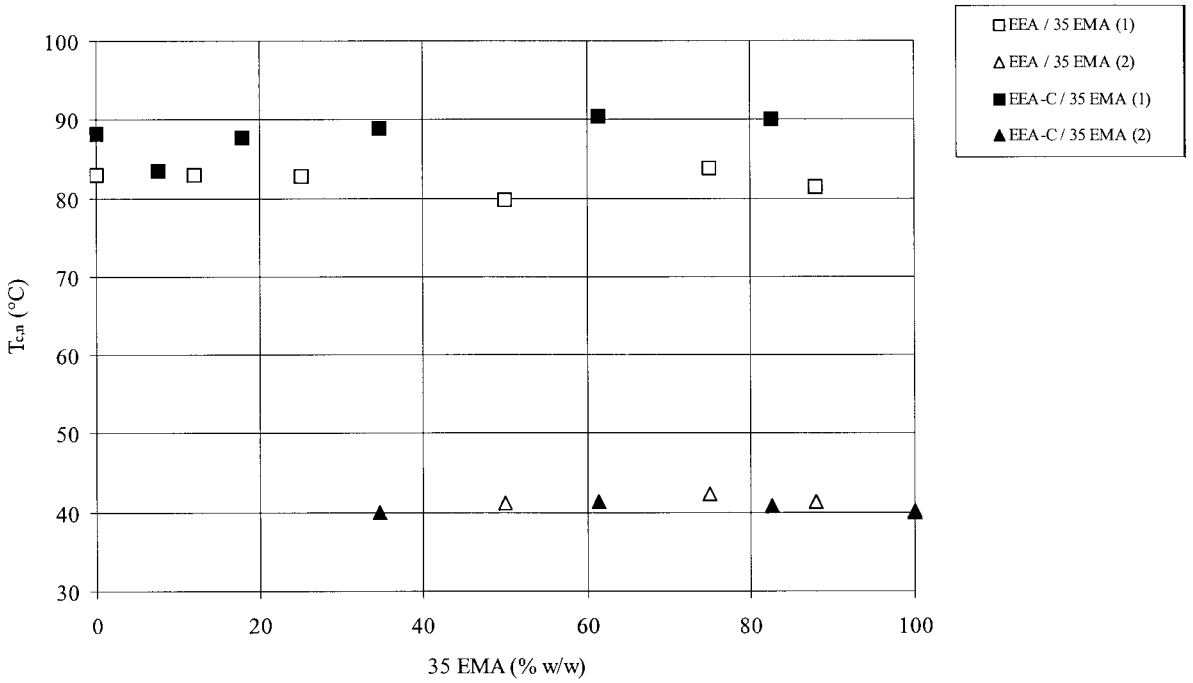

Figure 8 Nonisothermal crystallization temperature evolution in 35EMA/EEA blends with and without CB.

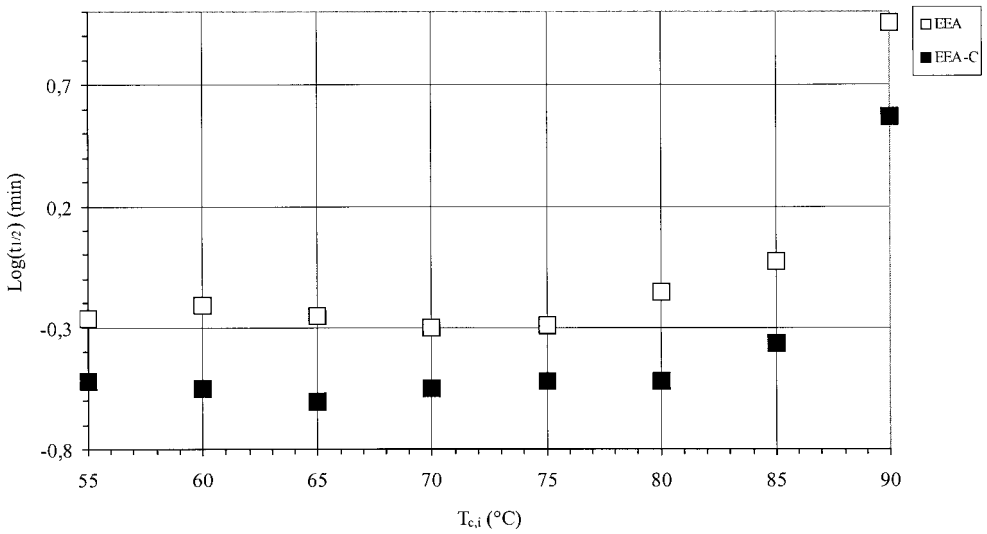

Figure 9 Half-crystallization time, $t_{1/2}$, expressed versus isothermal crystallization temperature, $T_{c,i}$, for EEA and EEA-C.

In the logarithmic scale, the kinetic difference between EEA and EEA-C is quite constant for $T_{c,i}$ higher than 55°C, whereas for T_c lower than 55°C, $t_{1/2}$ could not be determined accurately, because no quench treatment could be effective enough to prevent nonisothermal crystallization.

The modification of the isothermal and nonisothermal crystallization by CB might be attributed to interactions between the CB and the copolymer chains.

EEA Subsequent Melting Temperature

Isothermal crystallization offers a good opportunity to characterize the molecular distribution of EEA provided that the subsequent melting is analyzed. Isothermal crystallizations are carried out by fast cooling from the melt to $T_{c,i}$ at -90°C min^{-1}. Figure 10 shows the multiple endotherms obtained for EEA using a 20°C min^{-1} heating rate after isothermal crystallization at 55, 60, 65, 70, 75, and 80°C and cooling to 15°C at -20°C min^{-1}. Two or three melting zones are evidenced for both EEA and EEA-C and are collected in Figure 11.

Plotting T_m versus $T_{c,i}$ (also called the Hoffman–Weeks treatment[20]) is generally used to determine the equilibrium melting temperature $T_m{}^0$ using eq (1):

$$T_m = T_m^0\left(1 - \frac{1}{\gamma}\right) + \frac{T_c}{\gamma} \qquad (1)$$

where γ is a parameter that depends on the lamella thickness. More precisely, $\gamma = |l|^*$, where l and l^* are the thickness of the grown crystallite and of the critical crystallite nucleus, respectively.[19]

Nevertheless, it has been recently pointed out[20] that eq. (1) correctly represents the experimental data only when the slope of the T_m versus $T_{c,i}$ plots is approximately of 0.5. This condition is not fulfilled here, so that we did not try to determine $T_m{}^0$ for EEA or EEA-C and just made some comments on the data.

Figure 11 shows positions of three families of endotherms (noted 1, 2, and 3 in the legend) corresponding to different types of crystals. The main endotherm (3) near 100°C does not change significantly with T_c, except for T_c = 100°C, where crystals of higher T_m (106°C) are formed in a small quantity. The second endotherm (2) often appears as a shoulder, the temperature of which is difficult to estimate (see Fig. 10) and follows T_c evolution. The third endotherm (1), also following T_c evolution, corresponds to low melting temperature crystals and is attributed to species which cannot crystallize during the isothermal step and support nonisothermal crystallization during the final cooling to 15°C.

We can conclude from Figure 11 that the two crystalline species evidenced by the endotherms (3) and (2) correspond to the crystallization of poly(ethylene-*co*-acrylate) chains, respectively, from the acrylate-poor comonomer fraction and the acrylate-rich comonomer fraction. This is consistent with the composition drifts probably encountered during EXA synthesis.[15–17] As endo-

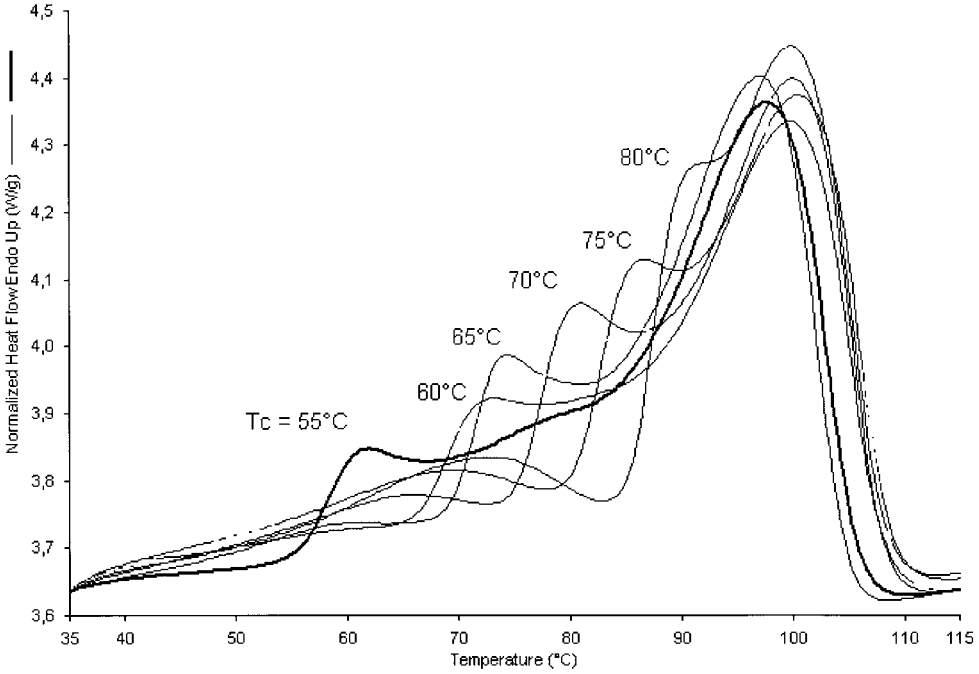

Figure 10 Typical DSC subsequent melting endotherms obtained for EEA at 20°C min^{-1} with $T_{c,i}$ from 55 to 80°C.

therms (1) and (2) seem to be divided by the $T_m = T_c$ line, it is likely that the isothermal step segregates chains during crystallization in terms of the crystallizable sequence mean length[18] ($\bar{l}_c$). As this segregation occurs on the whole T_c scale, the corresponding $\bar{l}_c$ distribution is expected to be

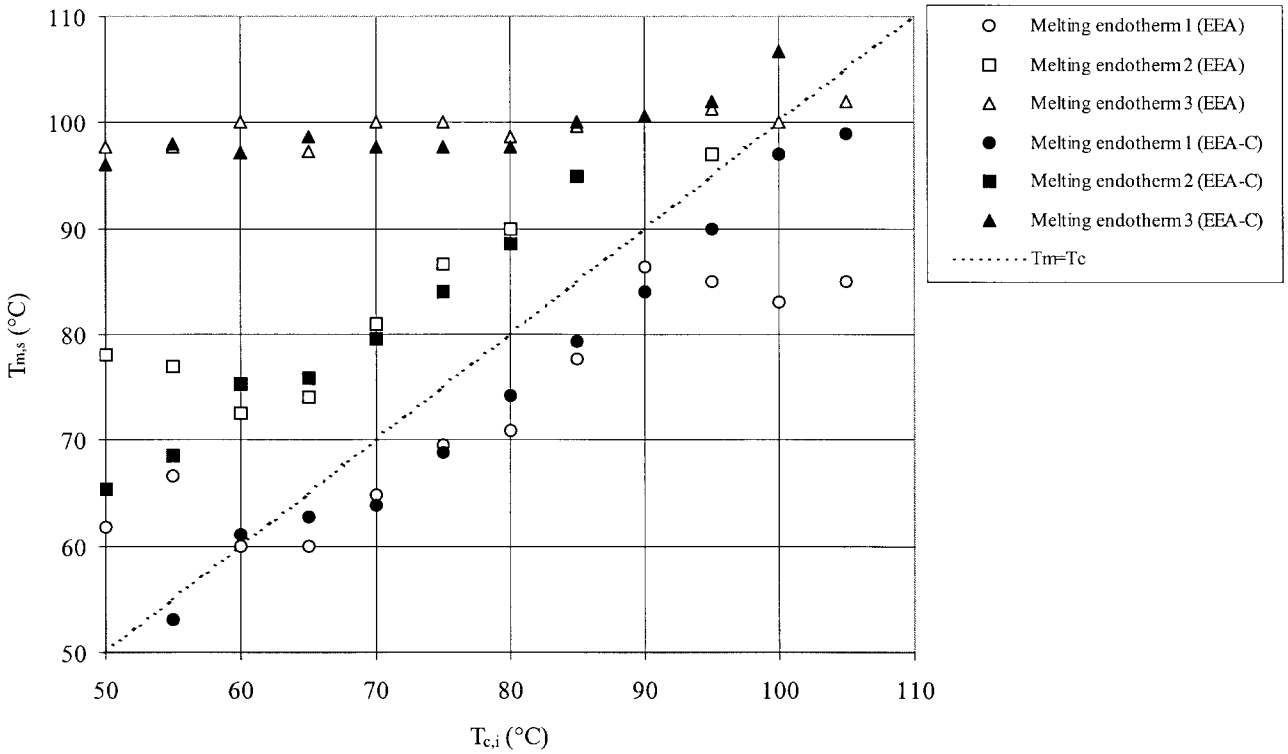

Figure 11 Subsequent melting temperature $T_{m,s}$ versus isothermal crystallization temperature $T_{c,i}$ for EEA and EEA-C. Dashed line represents $T_m = T_c$.

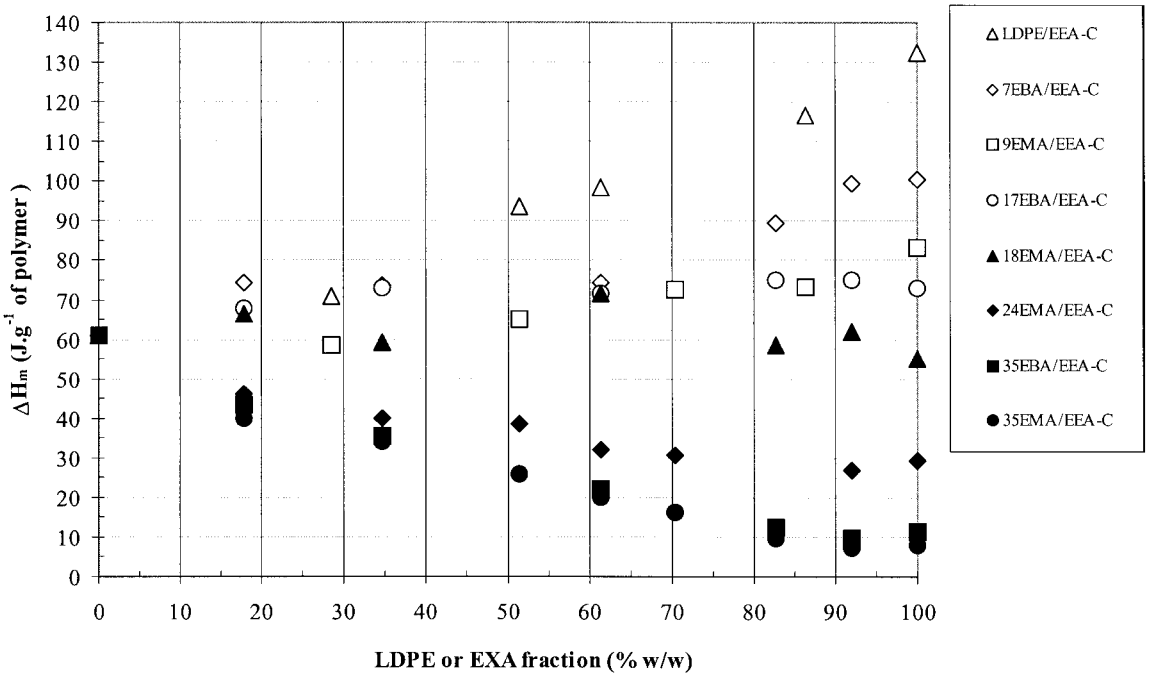

Figure 12 Influence of the alkyl acrylate content in the copolymer and EXA fraction in the EXA/EEA-C blends on the total melting enthalpy ΔH_m (J g^{-1}).

wide. Nevertheless, it is impossible to say whether the $\bar{l}_c$ distribution arises from molar mass or comonomer composition variations, although the latter proposition seems more probable.

The influence of CB on the EEA melting temperature does not seem to be very important. However, at high and low T_c, more regular variations of the subsequent melting temperature in the presence of CB can be noticed, illustrating, once more, its nucleating effect.

EEA-C/EXA Blends' Melting Enthalpy

The general evolution of the melting enthalpy of all the EEA-C/EXA blends is presented in Figure 12: (1) ΔH_m of the blend decreases with the alkyl acrylate content for a constant percentage of EXA because the acrylate comonomers are considered as defects toward crystallization; (2) for blends of EEA-C with EXAs more crystalline than EEA, ΔH_m increases with the EXA content; and (3) for blends of EEA-C with EXAs less crystalline than EEA, ΔH_m decreases with the EXA content.

At this point, it is interesting to compare the melting enthalpies of the EEA/EXAs and EEA-C/EXAs blends to determine the CB incidence. After the enthalpy values are corrected for CB %, the results are expressed in Figure 13 for EEA/24 EMA, EEA-C/24 EMA, EEA/35 EMA, and EEA-C/35 EMA blends. For blends without CB, ΔH_m follows quite well an additive law described by eq. (2), that is, the difference between the enthalpy calculated using eq. (2) and the DSC experimental value $\delta[\Delta H_m]$ is very weak. However, for blends containing CB, there is significant divergence from the additive law—$\delta[\Delta H_m]$ can reach 10 J $g^{-1}$of the polymer:

$$\Delta H_m = w_1 \Delta H_{m_1} + (1 - w_1)\Delta H_{m_2} \qquad (2)$$

where w_1 is the weight fraction. This phenomenon was already encountered with melt and solution-mixed high-density polyethylene/poly(propylene-*b*-ethylene) (HDPE/BPP blends).[29] The authors attributed the crystallinity decrease to a limitation caused by nucleation in the HDPE droplets dispersed in the BPP phase.

In the present work, $\delta[\Delta H_m]$ can clearly be interpreted in terms of CB interactions with the different polymers in the blend. To go further, it is useful to report $\delta[\Delta H_m]$ to ΔH_m (the melting enthalpy of the considered polymer crystallized without CB) to evaluate the incidence of CB on $\delta[\Delta H_m]$ for different alkyl acrylate percentages in the copolymers (Fig. 14).

It follows that CB interactions with the matrix increase with the acrylate content in EXA

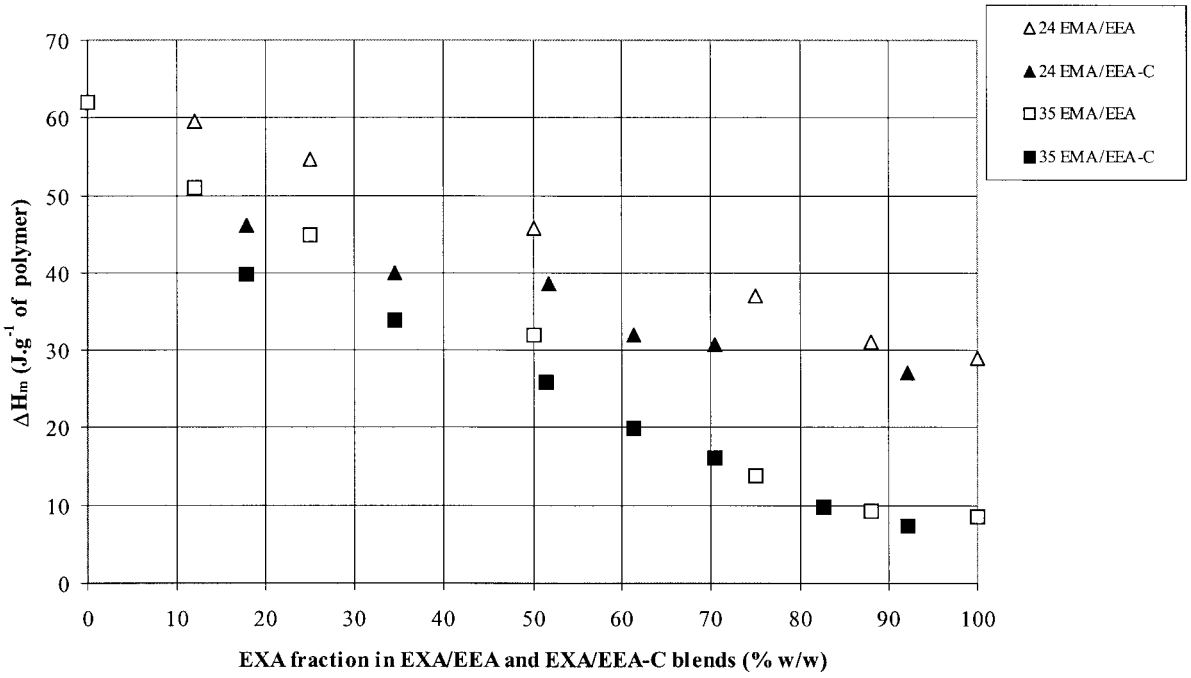

Figure 13 Melting enthalpies ΔH_m of EEA/24 EMA and EEA/35 EMA blends with and without CB function of the EXA fraction.

and with the CB content in the blend. In other words, there could be an increase of intermolecular interactions in the amorphous phase, which reduces the ability of some chains to crystallize and is responsible for the crystallinity loss. It has been pointed out from a theoretical point of view[30] that the introduction of a filler in a binary miscible or immiscible polymer mixture increased the thermodynamic stability of the ternary system.

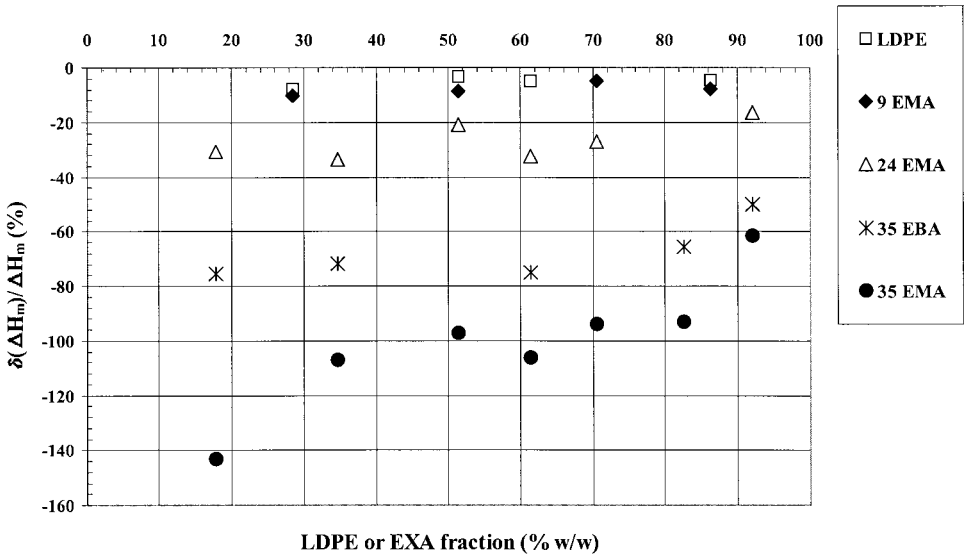

Figure 14 Normalized melting enthalpy differences $\delta(\Delta H_m)/\Delta H_m$ versus EXA fraction, for blends with LDPE, 9EMA, 24EMA, 35EMA, and 35EBA. $\delta(\Delta H_m)/\Delta H_m$ represents the melting enthalpy decrease in the presence of CB divided by the blend melting enthalpy without CB.

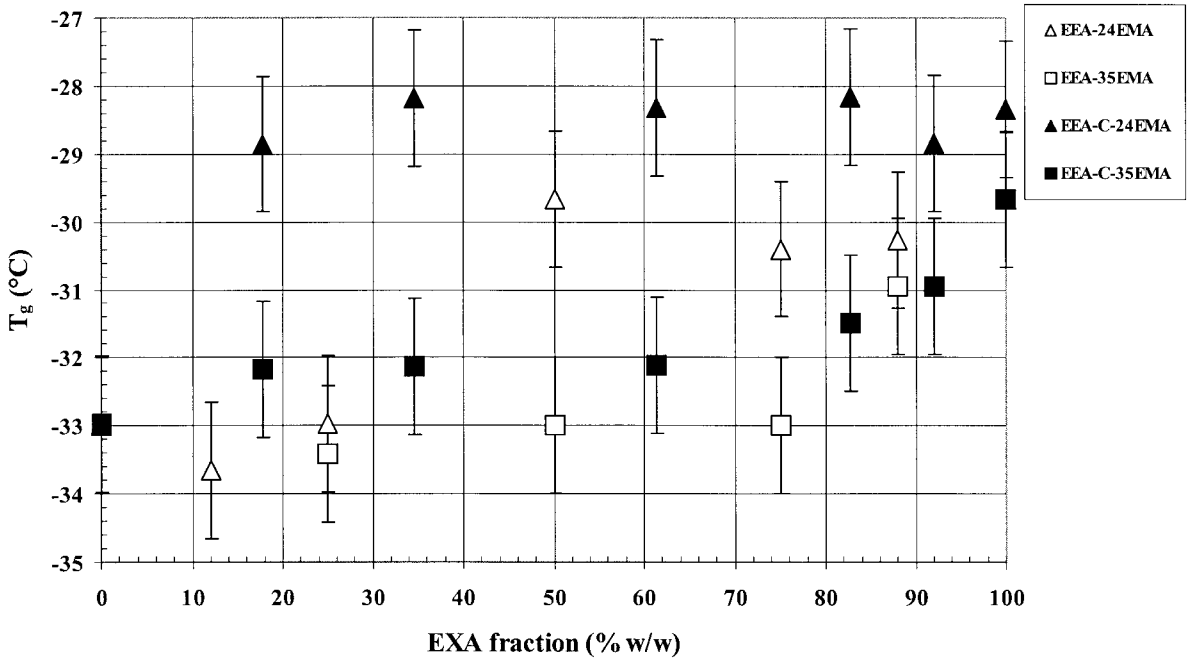

Figure 15 Influence of CB on the T_g of EEA/24EMA and EEA/35EMA blends.

Influence of CB on the Amorphous-phase Properties

As has been shown previously, CB is thought to develop interactions with the acrylate ester groups in the amorphous phase and to decrease the ability of the acrylate-rich fraction chains to crystallize. We tried to find other indications in examining the amorphous-phase characteristic parameters such as the glass transition temperature (T_g) and the specific heat variation through the glass transition (ΔC_p).

Blends' Glass Transition Temperature

As appears in Figure 15, the T_g's of EEA and EXA are very close and this makes it difficult to bring evidence of EXA's compatibility through a mixing law such as the Fox relation[31] expressed by eq. (3):

$$\frac{1}{T_g} = \frac{w_1}{T_{g_1}} + \frac{w_2}{T_{g_2}} \tag{3}$$

where w_1 and w_2 are the respective weight fractions. Thus, only one T_g could be detected and no shoulder could be seen on the sigmoid curves even with blends close to 50/50 (w/w), allowing us to suspect a good compatibility of the polymers in the amorphous phase. Another miscibility indication is deduced from the quite similar chemical structures of the components. Moreover, a slight increase of T_g in the presence of CB was observed (Fig. 15), more important for 24EMA-containing blends (from 1 to 4°C) than for 35EMA-containing blends (from 1 to 2°C), suggesting CB associations with macromolecules. This T_g increase is found to be nearly independent of the blend composition.

Heat-capacity Increment at Glass Transition Temperature (ΔC_p)

Plotting the heat-capacity increment through the glass transition (ΔC_p) versus the melting enthalpy (ΔH_m) allows, by extrapolation to $\Delta C_p = 0$, $\Delta H_m{}^0$ to be determined.[19,32] It can be seen in Figure 16 that the linear-regression slope is increased by the presence of CB. This means that for the same ΔH_m the ΔC_p is lower in CB-filled samples, suggesting there is some kind of rigid amorphous phase not contributing to the glass transition, probably due to interactions between alkyl acrylate groups and CB.

CONCLUSIONS

Two parameters were found to be of importance in this study on CB/poly(ethylene-*co*-alkyl acrylate) blends: the acrylate comonomer content and the CB content.

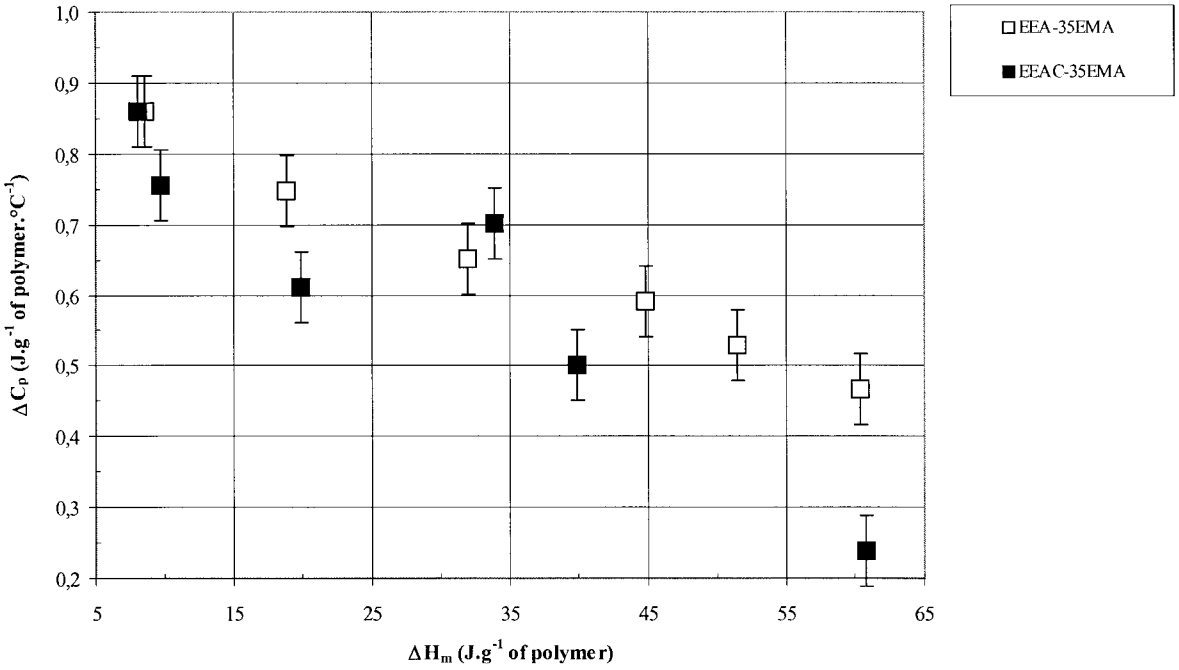

Figure 16 Evolution of ΔC_p with ΔH_m for EEA/35EMA blends with and without CB.

1. The acrylate comonomer content has several effects on the crystalline characteristic parameters of the studied polymer blends. An increase in the acrylate content leads to decrease of the melting enthalpy ΔH_m of the melting temperature T_m and of the nonisothermal crystallization temperature $T_{c,n}$. This is not surprising since the introduction of comonomers in a regular polymer chain generally leads to a decrease of the crystalline properties. The synthesis of ethylene/alkyl acrylate copolymers provides different families of chains of different molar masses and different acrylate content. The isothermal crystallization study confirms these data and shows a chain segregation according to their acrylate content, especially in the acrylate-rich fraction leading to different crystalline phases of different melting temperatures. The acrylate comonomer's poor fraction may first crystallize, hindering the crystallization of the rich fraction at lower temperatures. Such phase segregation must also operate during aging of these polymer blends, suggesting that a further study will have to investigate the time dependence of physical properties in such blends.
2. The CB presence in the blends has several effects on both the crystalline and amorphous characteristic parameters of the studied polymers (taken alone or in blends). There is an acceleration of both isothermal and nonisothermal crystallization of EEA in blends containing 24EMA and 35EMA. A decrease of the melting enthalpy of the EEA/EXA blends is also observed. The amorphous phase stiffness slightly increases.

These results make possible several propositions:

(a) The CB-induced crystallization rate enhancement of the acrylate-poor fraction, more than a pure nucleating effect, might be due to a selective adsorption of acrylate-rich chains. CB may also slow down the acrylate-rich chains' crystallization by an increase of the molecular interactions with the ester functions, thus decreasing the blends crystallinity.
(b) CB stays mainly in the amorphous phase even after the rich acrylate fraction has crystallized. This hypothesis seems realistic since crystals generally reject impurities like CB particles. Moreover, the acrylate comonomers have also an important probability not to enter the crystals, and if CB really interacts with the ester func-

tions, that increases the probability to find CB in the amorphous phase.

(c) Thus, the whole crystallization process may be described as follows: (1) The copolymer of higher crystallinity (of lower acrylate content) first crystallizes, rejecting CB and the amorphous phase of the lower crystallinity copolymer, and (2) the second copolymer crystallizes, rejecting, once more, CB in the amorphous phase with the noncrystallizable chains.

(d) At the end of the crystallization process, the morphology of the CB conductive pathway gives interesting conductive properties.

These blends of poly(ethylene-*co*-alkyl acrylate) copolymers with CB particles provide interesting morphologies that give materials with adjustable conductive properties which are a function of the acrylate and CB contents. The mechanical behavior and the conductive properties of such materials will be examined in a further study.

The authors thank Yann Dixneuf, Gérard Guévelou, and Chantal Bonnans for their contribution to this work. The Laboratoire Polymères & Procédés is under contract with the French Ministry of Research (UPRES No. 2592).

REFERENCES

1. Kohler, F. U.S. Patent 3 243 753, 1966; pp 1–8.
2. Bueche, F. J Appl Phys 1973, 44, 532–533.
3. Meyer, J. Polym Eng Sci 1973, 13, 462–468.
4. Meyer, J. Polym Eng Sci 1974, 14, 706–716.
5. Narkis, M.; Ram, A.; Flashner, F. Polym Eng Sci 1978, 18, 649–653.
6. Boulic, F.; Brosseau, C.; Le Mest, Y.; Loaëc, J.; Carmona, F. J Phys D Appl Phys 1998, 31, 1904–1912.
7. Yu, G.; Zhang, M. Q.; Zeng, H. M. J Appl Polym Sci 1998, 70, 559–566.
8. Narkis, M.; Ram, A.; Flashner, F. J Appl Polym Sci 1978, 22, 1163–1165.
9. Yi X.-S.; Wu, G., Ma, D. J Appl Polym Sci 1998, 67, 131–138.
10. Tang, H.; Chen, X.; Luo, Y. Eur Polym J 1997, 33, 1383–1386.
11. Lee, J. C.; Hikehara, T.; Nishi, T. J Appl Polym Sci 1998, 69, 193–199.
12. Zhang, M. Q.; Yu, G.; Zeng, H. M.; Zang, H. B.; Hou, Y. H. Macromolecules 1998, 31, 6724–6726.
13. Luo, Y.; Wang, G.; Zhang, B.; Zhang, Z. Eur Polym 1998, 34, 1221–1227.
14. Gubbels, F.; Jérôme, R.; Teyssié, P.; Vanlathem, E.; Deltour, R.; Calderone, A.; Parenté, V.; Brédas, J. L. Macromolecules 1994, 27, 1972–1974
15. Buback, M.; Busch, M.; Lovis, K. Macromol Chem Phys 1996, 197, 303–313.
16. Buback, M.; Dröge, T.; Van Herk, A.; Mähling, F. O. Macromol Chem Phys 1996, 197, 4119–4134.
17. Buback, M.; Dröge, T. Macromol Chem Phys 1997, 198, 3627–3638.
18. Feller, J. F.; Chabert, B.; Guyot, A.; Gérard, J. F.; Spitz, R. Compos Interf 1995, 3, 121–134.
19. Righetti, M. C.; Pizzoli, M.; Lotti, N.; Munari, A. Macromol Chem Phys 1998, 199, 2063–2070.
20. Hoffman, J. D.; Weeks, J. J. J Res Natl Bur Stand A 1962, 66, 13.
21. Feller, J. F.; Chabert, B.; Guyot, A.; Spitz, R.; Wagner, H. D.; Gérard, J. F. J Adhes 1996, 58, 299–313.
22. Miller R.L. In Encyclopedia of Polymer Science and Technology: Wiley: New York, 1966; Vol. 4, pp 449–528.
23. Devaux, E.; Chabert, B. Polym Commun 1991, 31, 391–394.
24. Mandelkern, L.; Mac Laughlin, K. W.; Alamo, R. G. Macromolecules 1992, 25, 1440–1444.
25. Tashiro, K.; Stein, R. S.; Hsu, S. L. Macromolecules 1992, 25, 1801–1808.
26. Gallagher, K. P; Zhang, X.; Runt, J. P.; Huynh-Ba, G.; Lin, J. S. Macromolecules 1993, 26, 588–596.
27. Tashiro, K.; Izushi, M.; Kobayashi, M.; Stein, R. S. Macromolecules 1994, 27, 1221–1227.
28. Zimmermann H. J. J Macromol Sci Phys 1993, 32, 141–161.
29. Feng, Y.; Jin, X.; Hay, J. N. J Appl Polym Sci 1998, 69, 2469–2475.
30. Nesterov, A. E.; Lipatov, Y. S. Polymer 1999, 40, 1347–1349.
31. Fox, T. G. Bull Am Phys Soc 1956, 1, 123.
32. Wunderlich, B. Thermal Characterization of Polymeric Materials: The Basis of Thermal Analysis, 2nd ed.; Turi, E. A., Ed.; Academic: New York, 1997; Vol. 1, p 385.